10616 *Biochemistry* **2010,** *49,* 10616–10622
DOI: 10.1021/bi1010305

BIOCHEMISTRY
including biophysical chemistry & molecular biology
*Article*

# Oxidation of Histidine Residues in Copper−Zinc Superoxide Dismutase by Bicarbonate-Stimulated Peroxidase and Thiol Oxidase Activities: Pulse EPR and NMR Studies[†]

Karunakaran Chandran,[‡] John McCracken,[§] Francis C. Peterson,[∥] William E. Antholine,[‡] Brian F. Volkman,[∥] and Balaraman Kalyanaraman*[,‡]

[‡]*Department of Biophysics, Free Radical Research Center, Medical College of Wisconsin, Milwaukee, Wisconsin 53226, United States,* [§]*Department of Chemistry, Michigan State University, East Lansing, Michigan 48824, United States, and* [∥]*Department of Biochemistry, Medical College of Wisconsin, Milwaukee, Wisconsin 53226, United States*

*Received June 28, 2010; Revised Manuscript Received October 29, 2010*

ABSTRACT: In this work, we investigated the oxidative modification of histidine residues induced by peroxidase and thiol oxidase activities of bovine copper−zinc superoxide dismutase (Cu-ZnSOD) using NMR and pulse EPR spectroscopy. 1D NMR and 2D-NOESY were used to determine the oxidative damage at the Zn(II) and Cu(II) active sites as well as at distant histidines. Results indicate that during treatment of SOD with hydrogen peroxide ($H_2O_2$) or cysteine in the absence of bicarbonate anion ($HCO_3^-$), both exchangeable and nonexchangeable protons were affected. Both His-44 and His-46 in the Cu(II) active site were oxidized based on the disappearance of NOESY cross-peaks between CH and NH resonances of the imidazole rings. In the Zn(II) site, only His-69, which is closer to His-44, was oxidatively modified. However, addition of $HCO_3^-$ protected the active site His residues. Instead, resonances assigned to the His-41 residue, 11 Å away from the Cu(II) site, were completely abolished during both $HCO_3^-$-stimulated peroxidase activity and thiol oxidase activity in the presence of $HCO_3^-$. Additionally, ESEEM/HYSCORE and ENDOR studies of SOD treated with peroxide/Cys in the absence of $HCO_3^-$ revealed that hyperfine couplings to the distal and directly coordinated nitrogens of the His-44 and His-46 ligands at the Cu(II) active site were modified. In the presence of $HCO_3^-$, these modifications were absent. $HCO_3^-$-mediated, selective oxidative modification of histidines in SOD may be relevant to understanding the molecular mechanism of SOD peroxidase and thiol oxidase activities.

Cu-ZnSOD,[1] a ubiquitous antioxidant enzyme present in the cytosol, nucleus, peroxisomes, and mitochondrial intermembrane space of eukaryotic cells, protects against superoxide anion-dependent oxidative damage (*1*, *2*). The superoxide dismutase (SOD) activity is responsible for catalytically converting superoxide to hydrogen peroxide (*3*). In the presence of high concentration of $H_2O_2$, SOD is slowly inactivated ($k = 3.1\ M^{-1}\ s^{-1}$) through formation of an active enzyme-bound oxidant, SOD−Cu(II)−$^{\bullet}$OH. The proposed mechanism for peroxidase activity is (*4*−*7*)

$$\text{SOD}-\text{Cu(II)} + H_2O_2 \rightarrow \text{SOD}-\text{Cu(I)} + O_2^{\bullet -} + 2H^+ \quad (1)$$

$$\text{SOD}-\text{Cu(I)} + H_2O_2 \rightarrow \text{SOD}-\text{Cu(II)}-{}^{\bullet}OH + OH^- \quad (2)$$

The reactivity of the SOD−Cu(II)−$^{\bullet}$OH was suggested to be similar to that of a "site-specific copper-bound hydroxyl radical" (*4*−*7*). The inactivation of the enzyme was attributed to the oxidation of a histidine residue bound to the copper atom at the active site, forming an imidazole radical that underwent further oxidation to 2-oxohistidine (*8*−*10*). The peroxidatic inactivation of SOD was mitigated by anionic, peroxidase substrates (formate, urate, azide, and nitrite) that have access to the active site of SOD, facilitated by the favorable electrostatic interaction (*11*−*14*).

Bicarbonate ($HCO_3^-$), a ubiquitous anion present in high concentrations (~25 mM) in biological systems, stimulates SOD peroxidase activity. Proposed mechanisms (eqs 1−3) suggest that $HCO_3^-$ enters the active site of SOD through a narrow channel and undergoes oxidation at the active site in the presence of $H_2O_2$ or cysteine to form the carbonate anion radical, $CO_3^-$, that diffuses out of the active site and oxidizes other substrates in the bulk solution (*11*−*14*).

$$\text{SOD}-\text{Cu(II)}-{}^{\bullet}OH + HCO_3^- \rightarrow \text{SOD}-\text{Cu(II)} + CO_3^{\bullet -} + H_2O \quad (3)$$

Using direct electron paramagnetic resonance (EPR) and electron nuclear double resonance (ENDOR) techniques, we have previously shown that the Cu(II) active site is not affected during $HCO_3^-$-mediated enhanced peroxidase activity (*15*). More recently, it was shown that $CO_2$ is a potential reactant leading to the formation of $CO_3^{\bullet -}$ during the peroxidase activity (*17*). In addition to the dismutase and peroxidase activities, SOD was also shown to autoxidize thiols in the presence of air to generate hydrogen peroxide via thiol oxidase activity (*16*).

To obtain a better understanding of the interaction between the histidine ligands and the oxidant generated at the active site of copper during $HCO_3^-$-stimulated SOD peroxidase/oxidase

[†]This work was supported by NIH Grants P41RR001008 and R01 NS040494.

*To whom correspondence should be addressed: 414-456-4000 (telephone); 414-456-6512 (fax); balarama@mcw.edu (e-mail).

[1]Abbreviations: 2D-NOESY, two-dimensional nuclear Overhauser effect spectroscopy; CD, circular dichroism; $CO_3^{\bullet -}$, carbonate radical anion; Cu-ZnSOD, copper−zinc superoxide dismutase; ENDOR, electron nuclear double resonance; EPR, electron paramagnetic resonance; ESEEM, electron spin echo envelope modulation; $H_2O_2$, hydrogen peroxide; $HCO_3^-$, bicarbonate anion; HYSCORE, hyperfine sublevel correlation; SOD, superoxide dismutase.

 Published on Web 11/01/2010 

activities, we used NMR and pulse EPR spectroscopy techniques, electron spin echo envelope modulation (ESEEM), and hyperfine sublevel correlation (HYSCORE). Both 1D NMR and NOESY techniques were used to investigate the oxidative damage of histidines at the diamagnetic Zn(II) as well as the paramagnetic Cu(II) active site and at sites away from the coordination sphere of the active sites. ESEEM was used to determine the changes in the magnetic parameters of coordinated nitrogen (to active site copper and zinc) and distal nitrogens of both nonbridged and bridged histidine residues.

## EXPERIMENTAL PROCEDURES

*Materials*. Bovine Cu-ZnSOD was obtained from Roche Diagnostics. Cysteine, deuterium oxide, hydrogen peroxide, sodium bicarbonate, sodium hydrogen phosphate, and DTPA were purchased from Sigma (St. Louis, MO, USA).

*NMR Measurements*. All $^1$H NMR experiments were performed on a Bruker 600 MHz spectrometer operating at 14.1 T. The solvent $H_2O$ resonance was suppressed using a 3-9-19 watergate scheme (*18*). 2D-NOESY spectra were collected using a mixing time of 150 ms. The 2D experiments were performed in phase-sensitive mode, using the time-proportional phase-increment method. A total of 512 free induction decays were collected using the 2K data points. Data were multiplied by a phase-shifted squared sine bell along both dimensions. Zero filling in the $f_1$ dimension was applied to obtain a matrix of 2K × 1K data points.

*Pulse EPR Measurements*. A typical reaction mixture (200 $\mu$L) for EPR measurements contained SOD (1.0 mM), $H_2O_2$ (5 mM), and $HCO_3^-$ (50 mM) in a phosphate buffer (100 mM, pH 7.4) containing DTPA (100 $\mu$M). Incubation mixtures were then transferred to a 4 mm quartz EPR tube (Wilmad) and frozen immediately in liquid nitrogen for pulsed EPR analysis. Pulse EPR data were collected on a Bruker E-680X spectrometer operating at X-band and equipped with a model ER4118X-MD-4-W1 probe and employing a 4 mm dielectric resonator. The sample temperature was maintained at 10 K using an Oxford Instrument liquid helium flow system equipped with a CF-935 cryostat and an ITC-503 temperature controller. ESEEM data were collected using a three-pulse, stimulated echo sequence (90°$-t-$90°$-T-$90°) with 90° microwave pulse widths of 16 ns (full width at half-maximum) and peak powers of 250 W (*19*). A four-step phase cycling sequence, $(+x, +x, +x)$, $(-x, +x, +x)$, $(+x, -x, +x)$, $(-x, -x, +x)$, together with the appropriate addition and subtraction of the integrated spin echo intensities served to remove the contributions of two-pulse echoes and baseline offsets from the data. An integration window of 24 ns was used to acquire the spin echo amplitudes, using the data set length of 512 points. ESEEM data were tapered with a Hamming window, and the Fourier-transformed ESEEM spectra were obtained by taking the absolute value of the Fourier transforms.

*ENDOR Measurements*. The X-band ENDOR spectra were recorded on a Bruker E500 ELEXYS spectrometer using an ENDOR/triple accessory (Bruker) cavity. ENDOR spectra were recorded by fixing the magnetic field at an EPR resonance and by applying partially saturating microwave power while sweeping the NMR transition with a radio-frequency (RF) source. The samples were prepared as in pulse EPR measurements.

$^1$H and $^{14}$N ENDOR spectra were recorded at 8 K at the indicated field positions. The EPR spectrum was partially saturated with 6.33 mW (15 dB) of microwave power, and the ENDOR spectra were recorded at 9.47 GHz with a 200 kHz modulation depth, 100 W radio-frequency power, and 1300 scans at field position I and 4500 scans at field position III, respectively.

*Circular Dichroism Measurements*. The CD spectra of SOD (10 $\mu$M) treated with $H_2O_2$ (100 $\mu$M) in the presence and absence of $HCO_3^-$ (25 mM) were recorded on a Jasco 710 CD spectropolarimeter in 0.1 cm quartz cuvettes, accumulated eight times, and corrected for the corresponding buffer using 1 nm bandwidth.

## RESULTS

*NMR Characterization of Oxidized Histidines during Peroxidase and Thiol Oxidase Activity of SOD: Protective Effect of $HCO_3^-$*. The changes in the histidine residues coordinated to copper(II) located at the active site and at distant sites during $HCO_3^-$-induced SOD peroxidase activity were investigated using NMR techniques. 1D NMR and $^1$H$-^1$H NOESY spectra show the effect of $H_2O_2$/cysteine on histidine modification of SOD during peroxidase and thiol oxidase activities. The exchangeable N−H proton resonances observed by 1D NMR and the cross-peaks between both exchangeable and nonexchangeable protons of various histidines detected by 2D NMR (Figure 1) were assigned according to Bertini et al. (*20*).

During peroxidase activity in the absence of $HCO_3^-$, the signals became weaker and broadened due to conformational heterogeneity resulting from oxidative damage to active site histidines (Figure 1B). In accordance with 1D NMR, the cross-peaks between NH and CH protons of H44 (labeled as 3 and 4), H46 (labeled as 5 and 7) belonging to the Cu(II) active site, and H69 (labeled 1 and 2) of Zn(II) are altered (Figure 1A,B). The oxidative damage of NH and CH protons of the H44 residue in close proximity with H69 of Zn(II) possibly alters H-bond interaction between them. The H-bond between NH of H69 and CO of Thr-135 is important in stabilizing the active site channel (*21*). Thr-135 belongs to the six-residue helix involved in the recognition and electrostatic guidance of the superoxide anion (*21*). However, in the presence of $HCO_3^-$, no significant changes occur to the Cu(II) active site histidine cross-peaks (Figure.1C). By contrast, in NOESY, the cross-peak labeled 6 due to H41 of N−H and C2−H was also abolished (Figure 1C, red circle with dashed lines). H41 (H$\varepsilon$2) is H-bonded to CO of Thr-39 (loop III) and H$\delta$1 to CO of H120 (loop VII) (*22*, *23*). The active site channel is formed by the electrostatic loop VII, where charged residues important in catalysis lie.

It has been reported that Cu-ZnSOD loses ~70% of its catalytic activity upon disruption of the Thr39-His43-His120 hydrogen bridge by altering the positions and orientations of catalytically essential Leu-38 and Arg-143 residues (*22*, *23*). In both the absence/presence of $HCO_3^-$, there is loss/reduction in Zn(II)-bound H69 cross-peaks. The absence of changes in the circular dichroism (CD) spectra during peroxidase/thiol oxidase activities reveals that oxidative damage does not destabilize the SOD tertiary structure (Figure 2). These findings suggest that $HCO_3^-$ can protect SOD from oxidative damage at the active site by diverting the diffusible oxidant (e.g., $CO_3^{\bullet-}$) to a distant amino acid residue.

$^1$H NMR and NOESY spectra of SOD during thiol oxidase activity in the absence of $HCO_3^-$ are similar to those of the control (Figure 3). However, in the presence of $HCO_3^-$, similar to that seen with SOD peroxidase activity, the H41 cross-peak labeled 6 was completely lost (Figure 3). Also, the 1D peaks b and d characteristic of H41 were abolished (Figure 3). The absence of oxidative damage in the absence of $HCO_3^-$ during thiol oxidase activity may be due to slow reaction of $H_2O_2$ with Cys (*24*). However, in the presence of

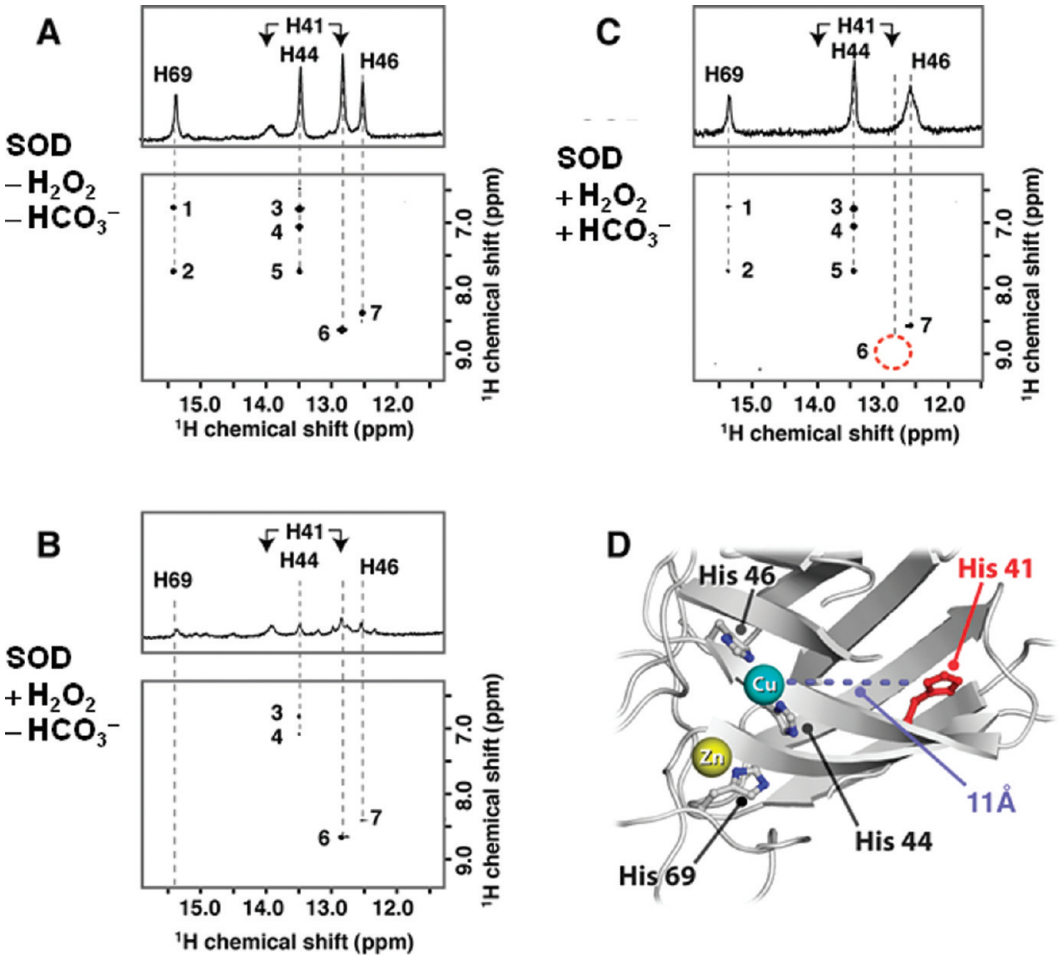


FIGURE 1: Effect of $HCO_3^-$ on oxidation of histidinyl residues of SOD: NMR studies. (A) 600 MHz $^1H-^1H$ NOESY and 1D NMR (as inset) spectra in $H_2O$ of SOD (1 mM) in 20 mM phosphate buffer (pH 7.4). (B) Same as (A) but in the presence of $H_2O_2$ (3 mM). (C) Same as (B) but in the presence of $HCO_3^-$ (50 mM). The labeled cross-peaks and 1D peaks are as follows: 1, H69 N−H and C4−H; 2, H69 N−H and C2−H; 3, H44 N−H and C2−H; 4, H44 N−H and C4−H; 5, H46 N−H and H69 C2−H; 6, H41 N−H and C2−H; 7, H46 N−H and C2−H and a, H46; b, H41; c, H44; d, H41(H3); e, H69. (D) Ribbon diagram of SOD (PDB ID 2SOD) showing the His-41 side chain oxidized in the presence of $HCO_3^-$ in red and active site His residues oxidized in the absence of $HCO_3^-$ in gray.

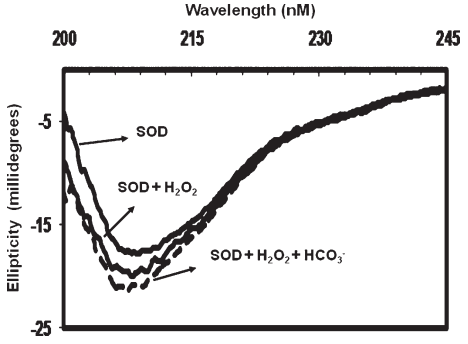


FIGURE 2: The CD spectra of SOD (10 $\mu$M) treated with $H_2O_2$ (100 $\mu$M) in the presence and absence of $HCO_3^-$ (25 mM) in phosphate buffer (50 mM, pH 7.4) containing DTPA (100 $\mu$M).

$HCO_3^-$, thiol oxidase activity stimulated SOD peroxidase activity leading to oxidative damage of other His residues.

*ESEEM Probing of Histidines Coordinated to Copper Site*. $^{14}N$-ESEEM spectra of SOD are typical of the remote nitrogens of histidyl imidazole ligands strongly bound to Cu(II). Figure 4A shows three-pulse time domain ESEEM data collected at $g = 2.06$ for SOD (black trace), SOD treated with $H_2O_2$ (red trace), and SOD treated with $H_2O_2$ in the presence of bicarbonate (green trace). The 1D-ESEEM spectrum for SOD is typical for $^{14}N$ near the exact cancellation condition showing sharp peaks at 0.6, 1.0, 1.3, and 1.6 MHz and a broader contribution with maxima at 4.1 and 4.5 MHz (Supporting Information Figure S1). The four-pulse HYSCORE spectrum for SOD (Figure 4B) is characterized by two sets of strong cross-peaks between $^{14}N$ double-quantum (dq-dq) transitions centered at (1.3, 4.0 MHz) and (1.6, 4.4 MHz) (*25*, *26*). Minor correlations between single-quantum and combination frequencies with the double-quantum transitions were also detected. These findings are in agreement with a previous ESEEM study of $^{15}N$-labeled SOD where two sets of nitrogen couplings were assigned to the four histidyl imidazole ligands bound to Cu(II) (*27*). Based on the previous report (*27*) the stronger hyperfine coupling, represented by the (1.6, 4.4 MHz) correlation in our HYSCORE spectra, was assigned to H44 and H46, while the weaker coupling, represented by the (1.3, 4.0 MHz) correlation, was assigned to H61 and H118.

ESEEM data collected for SOD treated with $H_2O_2$ show a 40% decrease in modulation depth (Figure 4A, red trace). Fourier transformation of these data shows narrow peaks at 0.4, 1.3, and 1.6 MHz and a broad double-quantum peak with an intensity maximum that stretches from about 3.8 to 4.2 MHz (Supporting Information Figure S2). The corresponding HYSCORE spectrum (Figure 4C) shows that the dominant $^{14}N$ dq-dq correlation is centered at (1.4,4.0 MHz) and extends over a frequency range from

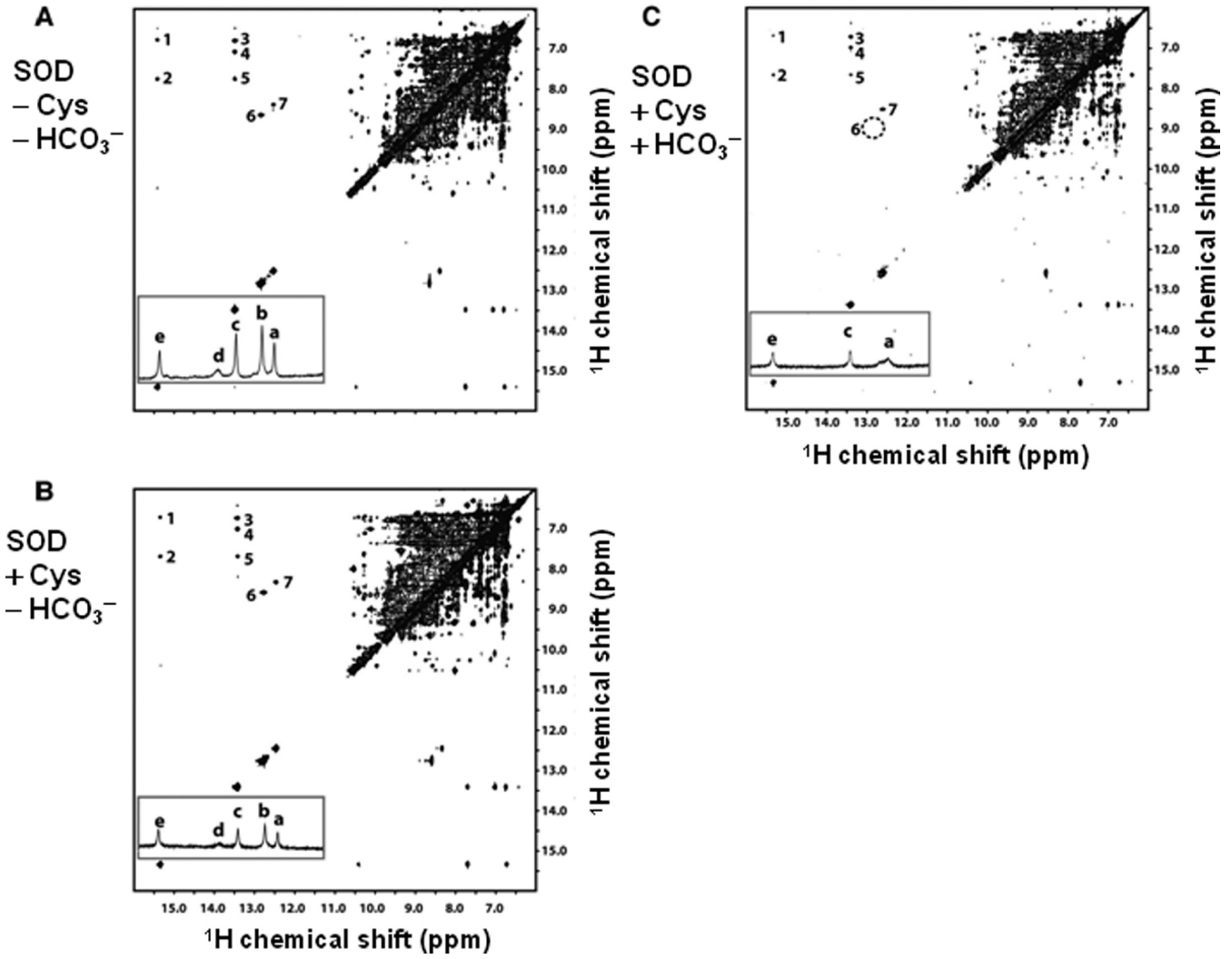


FIGURE 3: (A) 600 MHz $^1H-^1H$ NOESY and 1D NMR (as inset) spectra in 90% $H_2O$ and 10% $D_2O$ of Cu-Zn-SOD (1 mM) in 20 mM phosphate buffer (pH 7.4). (B) Same as (A) but incubated with cysteine (500 $\mu$M). (C) Same as (B) but incubated in presence of $HCO_3^-$ (50 mM) for 4 h. It was then followed by reduction of Cu(II) with 3 mM cysteine. Spectrometer conditions are described in the Experimental Procedures section. The cross-peaks and 1D peaks are labeled as follows: 1, H69 N−H and C4−H; 2, H69 N−H and C2−H; 3, H44 N−H and C2−H; 4, H44 N−H and C4−H; 5, H46 N−H and H69 C2−H; 6, H41 N−H and C2−H; 7, H46 N−H and C2−H and a, H46; b, H41; c, H44; d, H41(H3); e, H69.

3.5 to 4.3 MHz in the higher frequency dimension. A minor contribution at (1.5,4.4 MHz) is also detected (Figure 4C). SOD samples treated with $H_2O_2$ in the presence of $HCO_3^-$ showed three-pulse ESEEM (Figure 4A, green trace) and HYSCORE spectra (Figure 4D) that were identical to those detected for untreated SOD (Figure 4B).

*Probing of Copper−Histidine Coordination by ENDOR during SOD Thiol Oxidase Activity*. Proton ENDOR from histidines coordinated to Cu(II) were obtained at field positions I, II, and III indicated in Figure 5 (inset). $^1H$ and $^{14}N$ ENDOR spectra of SOD during thiol oxidase activity in the absence of $HCO_3^-$ reveal that resonances due to the coupled histidyl protons at the Cu(II) active site were broadened and diminished (Figure 5). In contrast, the proton ENDOR spectra of SOD treated with cysteine in the presence of $HCO_3^-$ were nearly similar to that of SOD alone. These results are in agreement with our earlier reports (*15*). Figure 5B shows the $^{14}N$ ENDOR spectra from histidines liganded to Cu(II) of SOD treated with cysteine alone and with $HCO_3^-$. The spectra for field position I were simulated (Figure 5B, dotted line) using the previously published parameters (*28*). Analysis of the spectra for the $A_z$ direction revealed that there are two types of nitrogen signals, $N_z(1)$ His-44 and His-46 and $N_z(2)$ His-61 and His-118. However, the two values are overlapping at this orientation to give only a single set of lines, $N_z(1,2)$ (not shown). For the $A_x$ direction, two sets of $^{14}N$ signals (Nx(1) and Nx(2)) were used in the simulation as shown in Figure 5B at field position III. These findings led us to conclude that the copper-bound His is not affected significantly in the presence of cysteine and $HCO_3^-$. However, in the presence of cysteine alone, the triplet signal in the low-frequency region was considerably diminished (Figure 5B at field position I). The triplet signal arises from His-44 and His-46 nitrogens (*15*). These results suggest that $HCO_3^-$-derived oxidant does not significantly alter the Cu(II) active site geometry and histidine coordination as does cysteine alone.

## DISCUSSION

Nearly 35 years ago, Hodgson and Fridovich proposed that the reaction between $H_2O_2$ and SOD could generate a copper-bound hydroxyl radical (SOD−Cu(II)−$^{\bullet}$OH) that reacts with $HCO_3^-$ to form a diffusible oxidant, $CO_3^{\bullet-}$, that oxidized several peroxidatic substrates (ABTS, dichlorodihydrofluorescein, and others) outside of the active site (*4*, *7*, *11*−*13*). More recently, it

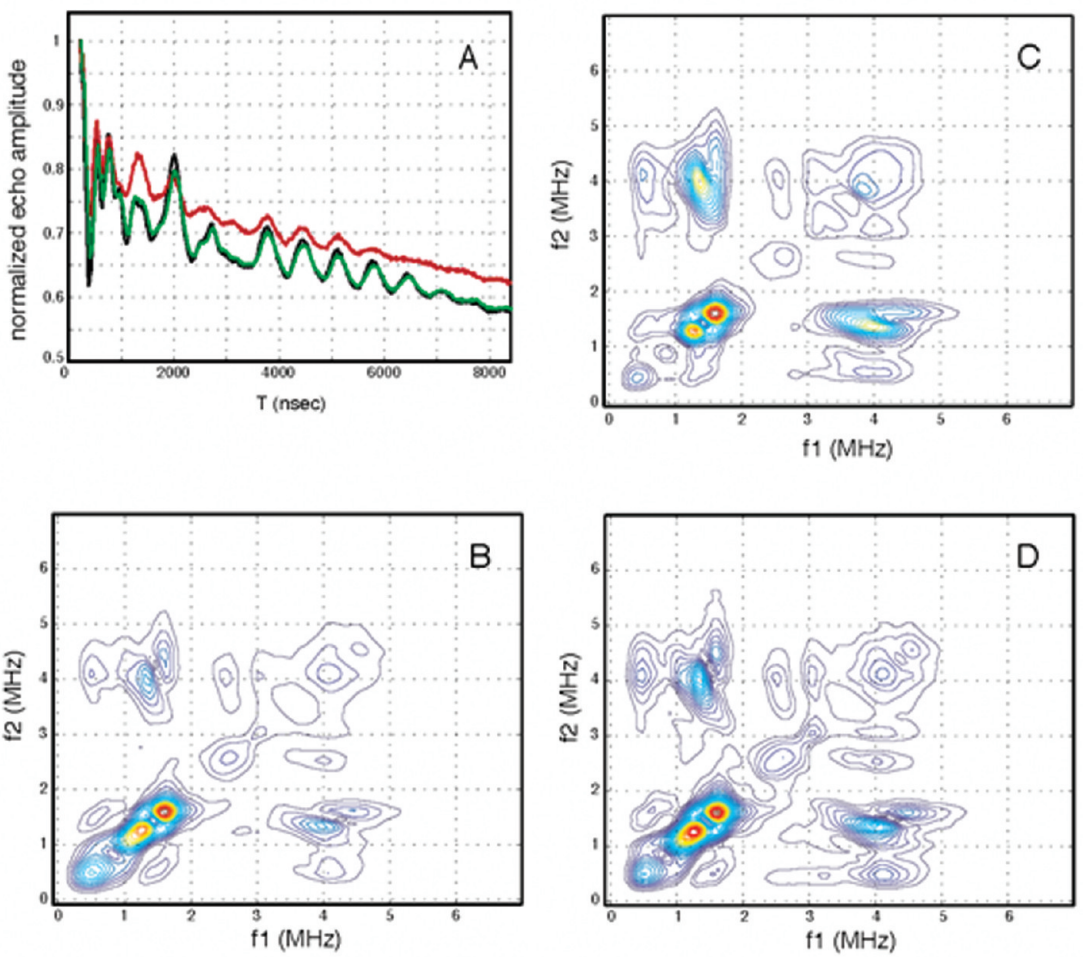


FIGURE 4: Three-pulse time domain ESEEM spectra (A) and four-pulse HYSCORE spectra collected for SOD in $H_2O$ in 100 mM phosphate buffer, pH = 7.4 (B), SOD treated with $H_2O_2$ (C), and SOD treated with $H_2O_2$ in the presence of $HCO_3^-$ (D). For (A), the black and green traces were collected for SOD and the SOD treated with $H_2O_2$ in the presence of $HCO_3^-$, respectively, while the red trace was collected for the SOD sample treated with $H_2O_2$. Conditions for data acquisition common to all data sets were as follows: microwave frequency, 9.681 GHz; magnetic field strength, 335.0 mT; tau value, 140 ns; sample temperature, 10 K. Pulse powers of equal amplitude were used for HYSCORE data acquisition.

was shown that $CO_2$, not $HCO_3^-$, undergoes peroxidation to $CO_3^{\bullet-}$ in the presence of $H_2O_2$ and SOD (*29*). Using EPR spin-trapping methods, evidence for $CO_3^{\bullet-}$ and other radicals derived from it was demonstrated during $HCO_3^-$-stimulated peroxidase activity of SOD (*11*, *30*). The oxidant derived from $HCO_3^-$ (i.e., carbonate anion radical) was proposed to react with surface-associated Trp-32 in human SOD forming a tryptophanyl radical (*31*). Mutation of Trp-32 by phenylalanine totally eliminated the Trp-32 radical formed from hSOD reaction with $H_2O_2$ and $HCO_3^-$ (*31*), providing additional evidence for the reaction between $CO_3^{\bullet-}$ and tryptophan-32 on the surface of the protein (*31*).

An alternative mechanism for $HCO_3^-$-mediated peroxidase activity has also been proposed. It was proposed that the active species (peroxycarbonate or $HCO_4^-$) formed during the peroxidase activity is enzyme-associated and nondiffusible (*32*). It was also suggested that the enzyme-associated oxidant ($HCO_4^-$, a nonradical) does not diffuse away from the active site but reacts locally at the active site of copper-bound histidines. The present magnetic resonance analyses clearly rule out the "enzyme-bound peroxycarbonate" as an oxidant responsible for oxidation of the "distant" histidine residues. The mechanism of direct oxidation of histidine at the active site by peroxycarbonate remains to be determined, however.

It was shown that SOD has a thiol oxidase activity (*16*). Previously, we proposed that $HCO_3^-$-stimulated peroxidase activity further accelerated thiol oxidase activity (*24*). Using a kinetic simulation model, the EPR profile changes in SOD−Cu(II) were simulated (*24*). Thiol oxidase activity generated *in situ* $H_2O_2$ needed for SOD peroxidase activity that was further stimulated by bicarbonate. The peroxidase activity enhanced thiol depletion and oxygen consumption resulting in increased thiol oxidase activity via formation of a diffusible $CO_3^{\bullet-}$ species.

The ESEEM experiment offers a sensitive means for viewing the structural relationship between Cu(II) and its four coordinated histidine ligands (*25*, *26*). In a HYSCORE experiment, the hyperfine coupling between Cu(II) and the remote nitrogen of a strongly bound histidyl imidazole ligand gives rise to cross-peaks near (1.5, 4.0 MHz) whose contours are parallel to the frequency axes. The HYSCORE spectrum of SOD at $g = 2.06$ (Figure 4B) shows two of these double-quantum, dq-dq, cross-peaks of nearly equal intensity that we can assign to a stronger set of hyperfine couplings due to H44 and H46 and a weaker set of couplings arising from H61 and H118 based on previous ESEEM studies (*27*). Treatment of the enzyme with $H_2O_2$ causes the ESEEM depth or amplitude to decrease by about 40%, and the dq-dq correlation in the HYSCORE spectrum (Figure 4C) is altered to show a more intense broader correlation centered at (1.4, 4.0 MHz) and a minor contribution at (1.6, 4.4 MHz). Previous studies of SOD treated with peroxide have shown that H118 is selectively oxidized to form a 2-oxohistidine species (9). Although the $^{14}$N-ESEEM amplitude is a function of the interplay between ligand hyperfine, nuclear

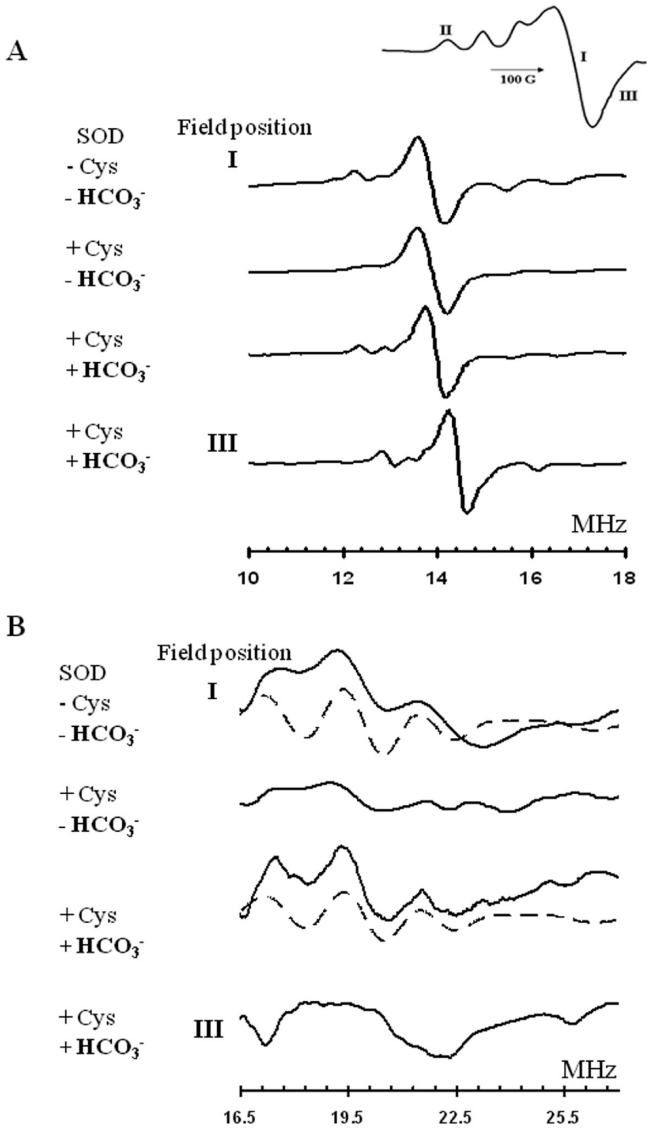


FIGURE 5: (A) X-band $^{1}$H ENDOR and (B) $^{14}$N ENDOR of SOD in the presence of cysteine (Cys) and/or $HCO_3^-$ at indicated field positions I and III of the EPR spectrum of SOD (inset). The SOD (1 mM) was incubated with cysteine (500 $\mu$M) for 4 h and repeated for five more times to equilibrate the cysteine concentration, 3 mM in 100 mM phosphate buffer, pH 7.4, with or without $HCO_3^-$ (50 mM) containing 100 $\mu$M DTPA at 8 K. Spectrometer conditions are described for the ENDOR measurements in the Experimental Procedures section.

Zeeman, and nuclear quadrupole interactions, the HYSCORE spectra show that the hyperfine coupling changes that result from peroxide treatment are minor. The 40% loss in ESEEM amplitude can only be explained by the loss of at least one Cu(II)−histidine hyperfine interaction, commensurate with the breaking of the Cu(II)−H118 bond. This bond-breaking chemistry then leads to the changes in hyperfine coupling for the remaining histidyl imidazole ligands that are captured in the HYSCORE cross-peak pattern centered at (1.4, 4.0 MHz). The previous biochemical studies that showed selective oxidation of H118 also showed that this modification only occurred in 66% of the Cu(II) sites. The residual cross-peak due to the stronger Cu(II)−histidine interaction in $H_2O_2$-treated SOD (Figure 4C) likely represents the fraction of Cu(II) sites where H118 is not oxidized and remains bound to Cu(II). Finally, the ESEEM data show conclusively that peroxide treatment in the presence of physiologically relevant levels of bicarbonate does not alter the ligation of H44, H46, H61, and H118 to Cu(II).

The present NMR study has limitations in that the 2D homonuclear NMR experiments using the commercially available protein enabled only the histidine analysis. The best way to confirm the structural assignments would have been to make recombinant SOD and the histidine mutants. To characterize the specific histidine modification, $^{15}$N-labeled recombinant SOD should be used. Lack of these studies clearly present a limited scope for detailed experimental interpretations on the oxidative modification.

The present data using the combined approach involving ESEEM/HYSCORE, ENDOR, and 1D NMR techniques are consistent with the previous mass spectral studies (*9*) indicating His118 oxidation during inactivation of Cu-ZnSOD with $H_2O_2$. The previous results also reported that histidine oxidation at other copper sites might be involved (*9*). The present magnetic resonance analyses also suggest marked changes in the hyperfine couplings at other copper(II)−histidine sites. These results reveal that the oxidation of His residues in Cu-ZnSOD in the presence of $H_2O_2$ alone is presumably more extensive. However, the NMR and ESEEM/HYSCORE results indicate that in the presence of bicarbonate the histidine oxidation is selective, occurring outside of the active site.

The present results are significant because $HCO_3^-$ is abundant in all living cells protecting SOD from its oxidative damage at the active site but causes extensive damage to outer residues of SOD or other vital proteins as observed in neurodegenerative diseases. A large body of evidence indicates that elevated oxidative stress perhaps due to peroxidase/thiol oxidase-stimulated peroxidase activity of SOD could play a major role in free radical biology. Finally, the combined use of NMR and EPR techniques is a powerful approach to elucidate the structural biological changes induced by site-specific generation of oxidants in biomolecules.

*Summary*. The combined NMR and pulse EPR data show that in the absence of $HCO_3^-$ the Cu(II) binding histidine residues were specifically oxidized and the other histidine residues were not affected during peroxidase and thiol oxidase activity of SOD. However, in the presence of $HCO_3^-$, the Cu(II)-bound histidines in SOD were unaffected; instead, a distant histidine residue (Figure 1D) was oxidized by a diffusible oxidant (most likely $CO_3^{\bullet-}$) formed at the active site of SOD.

## ACKNOWLEDGMENT

K.C. expresses thanks to the Managing Board, VHNSN College, Virudhunagar, India, for his sabbatical leave.

## SUPPORTING INFORMATION AVAILABLE

Additional ESEEM spectra of SOD alone and treated with $H_2O_2$. This material is available free of charge via the Internet at http://pubs.acs.org.

## REFERENCES

1. McCord, J. M., and Fridovich, I. (1969) Superoxide dismutase. An enzymic function for erythrocuprein (hemocuprein). *J. Biol. Chem. 244*, 6049–6055.
2. Okado-Matsumoto, A., and Fridovich, I. (2001) Subcellular distribution of superoxide dismutases (SOD) in rat liver: Cu,Zn-SOD in mitochondria. *J. Biol. Chem. 276*, 38388–38393.
3. McCord, J. M., and Fridovich, I. (1968) The reduction of cytochrome *c* by milk xanthine oxidase. *J. Biol. Chem. 243*, 5753–5760.
4. Fridovich, I. (1975) Suproxide dismutases. *Annu. Rev. Biochem. 44*, 147–159.

5. Fridovich, I. (1995) Superoxide radical and superoxide dismutases. *Annu. Rev. Biochem. 64*, 97–112.
6. Hodgson, E. K., and Fridovich, I. (1975) The interaction of bovine erythrocyte superoxide dismutase with hydrogen peroxide: chemiluminescence and peroxidation. *Biochemistry 14*, 5299–5303.
7. Hodgson, E. K., and Fridovich, I. (1975) The interaction of bovine erythrocyte superoxide dismutase with hydrogen peroxide: inactivation of the enzyme. *Biochemistry 14*, 5294–5298.
8. Sato, K., Akaike, T., Kohno, M., Ando, M., and Maeda, H. (1992) Hydroxyl radical production by $H_2O_2$ plus Cu,Zn-superoxide dismutase reflects the activity of free copper released from the oxidatively damaged enzyme. *J. Biol. Chem. 267*, 25371–25377.
9. Uchida, K., and Kawakishi, S. (1994) Identification of oxidized histidine generated at the active site of Cu,Zn-superoxide dismutase exposed to $H_2O_2$. Selective generation of 2-oxo-histidine at the histidine 118. *J. Biol. Chem. 269*, 2405–2410.
10. Uchida, K., and Kawakishi, S. (1990) Site-specific oxidation of angiotensin I by copper(II) and L-ascorbate: conversion of histidine residues to 2-imidazolones. *Arch. Biochem. Biophys. 283*, 20–26.
11. Zhang, H., Joseph, J., Gurney, M., Becker, D., and Kalyanaraman, B. (2002) Bicarbonate enhances peroxidase activity of Cu,Zn-superoxide dismutase. *J. Biol. Chem. 277*, 1013–1020.
12. Singh, R. J., Goss, S. P. A., Joseph, J., and Kalyanaraman, B. (1998) Nitration of $\gamma$-tocopherol and oxidation of $\alpha$-tocopherol by copper-zinc superoxide dismutase/$H_2O_2$/$NO_2^-$: role of nitrogen dioxide free radical. *Proc. Natl. Acad. Sci. U.S.A. 95*, 12912–12917.
13. Andrekopoulos, C., Zhang, H., Joseph, J., Kalivendi, S., and Kalyanaraman, B. (2004) Bicarbonate enhances $\alpha$-synuclein oligomerization and nitration: intermediacy of carbonate radical anion and nitrogen dioxide radical. *Biochem. J. 378*, 435–447.
14. Sankarapandi, S., and Zweier, J. L. (1999) Bicarbonate is required for the peroxidase function of Cu,Zn-superoxide dismutase at physiologic pH. *J. Biol. Chem. 274*, 1226–1232.
15. Karunakaran, C., Zhang, H., Crow, J. P., Antholine, W. A., and Kalyanaraman, B. (2004) Direct probing of copper active site and free radical formed during bicarbonate-dependent peroxidase activity of bovine and human copper, zinc superoxide dismutases: low-temperature electron paramagnetic resonance and electron nuclear double resonance studies. *J. Biol. Chem. 279*, 32534–32540.
16. Winterbourn, C. C., Peskin, A. V., and Parsons-Mair, H. N. (2002) Thiol oxidase activity of copper, zinc superoxide dismutase. *J. Biol. Chem. 277*, 1906–1911.
17. Liochev, S. I., and Fridovich, I. (2010) Mechanism of the peroxidase activity of Cu,Zn superoxide dismutase. *Free Radical Biol. Med. 48*, 1565–1569.
18. Sklenar, V., Piotto, M., Leppik, R., and Saudek, V. (1993) Gradient-tailored water suppression for $^1H$-$^{15}N$ HSQC experiments optimized to retain full sensitivity. *J. Magn. Reson., Ser. A 102*, 241–245.
19. Sharpe, M. A., Krzyaniak, M. D., Xu, S., McCracken, J., and Ferguson-Miller, S. (2009) EPR evidence of cyanide binding to the Mn(Mg) center of cytochrome *c* oxidase: support for Cu(A)-Mg involvement in proton pumping. *Biochemistry 48*, 328–335.
20. Bertini, I., Capozzi, F., Luchinat, C., Piccioli, M., and Viezzoli, M. S. (1991) Assignment of active-site protons in the $^1H$-NMR spectrum of reduced human Cu/Zn superoxide dismutase. *Eur. J. Biochem. 197*, 691–697.
21. Tainer, J. A., Getzoff, E. D., Richardson, J. S., and Richardson, D. C. (1983) Structure and mechanism of copper, zinc superoxide dismutase. *Nature 306*, 284–287.
22. Shipp, E. L., Cantini, F., Bertini, I., Valentine, J. S., and Banci, L. (2003) Dynamic properties of the G93A mutant of copper-zinc superoxide dismutase as detected by NMR spectroscopy: implications for the pathology of familial amyotrophic lateral sclerosis. *Biochemistry 42*, 1890–1899.
23. Toyama, A., Takahashi, Y., and Takeuchi, H. (2004) Catalytic and structural role of a metal-free histidine residue in bovine Cu-Zn superoxide dismutase. *Biochemistry 43*, 4670–4679.
24. Karunakaran, C., Zhang, H., Joseph, J., Antholine, W. E., and Kalyanaraman, B. (2005) Thiol oxidase activity of copper, zinc superoxide dismutase stimulates bicarbonate-dependent peroxidase activity via formation of a carbonate radical. *Chem. Res. Toxicol. 18*, 494–500.
25. Mims, W. B., and Peisach, J. (1978) The nuclear modulation effect in electron spin echos for complexes of $Cu^{+2}$ and imidazole with $^{14}N$ and $^{15}N$. *J. Chem. Phys. 69*, 4921–4930.
26. Kofman, V., Farver, O., Pecht, I., and Goldfarb, D. (1996) Two-dimensional pulsed EPR spectroscopy of the copper protein azurin. *J. Am. Chem. Soc. 118*, 1201–1206.
27. Dikanov, S., Felli, I., Viezzoli, M.-S., Spoyalov, A., and Hüttermann, J. (1994) X-band ESEEM spectroscopy of $^{15}N$ substituted native and inhibitor-bound superoxide dismutase. Hyperfine couplings with remote nitrogen of histidine ligands. *FEBS Lett. 345*, 55–60.
28. Reinhard, H., Kappl, R., Hütterman, J., and Viezzoli, M. S. (1994) ENDOR of superoxide dismutase: structure determination of the copper site from randomly oriented specimen. *J. Phys. Chem. 98*, 8806–8812.
29. Liochev, S. I., and Fridovich, I. (2004) $CO_2$, not $HCO_3^-$, facilitates oxidations by Cu,Zn superoxide dismutase plus $H_2O_2$. *Proc. Natl. Acad. Sci. U.S.A. 101*, 743–744.
30. Ramirez, D. C., Gomez Mejiba, S. E., and Mason, R. P. (2005) Mechanism of hydrogen peroxide-induced Cu,Zn-superoxide dismutase-centered radical formation as explored by immune-spin trapping: the role of copper- and carbonate radical anion-mediated oxidations. *Free Radical Biol. Med. 38*, 201–214.
31. Zhang, H., Andrekopoulos, C., Joseph, J., Karunakaran, C., Karoui, H., Crow, J. P., and Kalyanaraman, B. (2003) Bicarbonate-dependent peroxidase activity of human Cu,Zn-superoxide dismutase induces covalent aggregation of protein: intermediacy of tryptophan-derived oxidation products. *J. Biol. Chem. 278*, 24078–24089.
32. Elam, J. S., Malek, K., Rodriguez, J. A., Doucette, P. A., Taylor, A. B., Hayward, L. J., Cabelli, D. E., Valentine, J. S., and Hart, P. J. (2003) An alternative mechanism of bicarbonate-mediated peroxidation by copper-zinc superoxide dismutase: rates enhanced via proposed enzyme-associated peroxycarbonate intermediate. *J. Biol. Chem. 278*, 21032–21039.